

Blast vibration of a large-span high-speed railway tunnel based on microseismic monitoring

Ao Li, Qian Fang*, Dingli Zhang, Jiwei Luo and Xuefei Hong

Key Laboratory for Urban Underground Engineering of the Education Ministry, Beijing Jiaotong University, Beijing 100044, China

(Received December 8, 2017, Revised March 26, 2018, Accepted March 30, 2018)

Abstract. Ground vibration is one of the most undesirable effects induced by blast operation in mountain tunnels, which could cause negative impacts on the residents living nearby and adjacent structures. The ground vibration effects can be well represented by peak particle velocity (PPV) and corner frequency (f_c) on the ground. In this research, the PPV and the corner frequency of the mountain surface above the large-span tunnel of the new Badaling tunnel are observed by using the microseismic monitoring technique. A total of 53 sets of monitoring results caused by the blast inside tunnel are recorded. It is found that the measured values of PPV are lower than the allowable value. The measured values of corner frequency are greater than the natural frequencies of the Great Wall, which will not produce resonant vibration of the Great Wall. The vibration effects of associated parameters on the PPV and corner frequency which include blast charge, rock mass condition, and distance from the blast point to mountain surface, are studied by regression analysis. Empirical formulas are proposed to predict the PPV and the corner frequency of the Great Wall and surface structures due to blast, which can be used to determine the suitable blast charge inside the tunnel.

Keywords: microseismic monitoring; blast vibration; large-span tunnel; peak particle velocity; corner frequency

1. Introduction

When a mountain tunnel is excavated using the drilling and blast method, the vibration due to blast inevitably produces negative impacts on the surface structures (Ak *et al.* 2009, Nateghi 2012, Verma *et al.* 2018). The appropriate evaluation of the blast vibration is of fundamental importance in safeguarding the existing structures adjacent to tunnelling. The peak particle velocity (PPV) and the corner frequency are the two key parameters, commonly adopted to identify the blast vibration impacts on existing structures (Hasanipanah *et al.* 2017).

The peak particle velocity refers to the maximum speed of a particular particle as it oscillates about a point of equilibrium that is moved by a passing wave, which is proportional to the produced energy and dynamic stress due to blast (Faradonbeh *et al.* 2016). The PPV is one of the best descriptors for correlating case history data with vibration-induced damage (New 1986, Sharif 2000). Both the analytical solutions (Sambuelli 2009, Arora and Dey 2010) and empirical solutions (Sadovskii 1973, Jiang and Zhou 2012, Xia *et al.* 2018) have been proposed to calculate the PPV produced by blast. Numerical simulations (Saiang and Nordlund 2009, Verma *et al.* 2018) have also been used to obtain the PPV associated with blast. In addition, the artificial intelligence methods, including artificial neural networks, genetic algorithms, and fuzzy expert systems have been conducted to predict the PPV value (Dehghani and Atae-Pour 2011, Monjezi *et al.* 2011, Amnieh *et al.*

2012, Faradonbeh *et al.* 2016).

The corner frequency is defined by the frequency at which the high and low frequency trends intersect, which can be used to describe the predominant frequency due to blast vibration (Wyss *et al.* 1971, Sato and Hirasawa 1973). When the corner frequency is close to the natural frequency of the structure, it may produce resonant vibration, and the blast vibration effects will be aggravated (Dargahi-Noubary *et al.* 1998, Li *et al.* 2008). Related studies on corner frequency focus on the analysis of field measurement data (Yang *et al.* 2016). Several theoretical solutions are proposed to predict corner frequency (Aldas 2010, Lu *et al.* 2013).

The new Badaling tunnel is excavated below the Badaling Great Wall using the drilling and blast method. The ground vibration caused by blast may produce negative effects on the Great Wall. To assess the effects of the imposed vibration on the Great Wall, the microseismic monitoring technique is adopted to record the PPV and corner frequency on the mountain surface. The recorded PPV values caused by the current blast are lower than the guide value (0.3 cm/s), and the measured corner frequencies are larger than the natural frequencies of the Great Wall, which will not lead to resonant vibration of the Great Wall. Therefore, the vibration safety of the Great Wall due to the current blast can be ensured. Moreover, some empirical formulas are obtained by regression analysis, which can be used to predict the PPV and the corner frequency of the mountain surface due to blast inside the tunnel.

2. Project overview

The Beijing-Zhangjiakou high-speed railway project is

*Corresponding author, Professor
E-mail: qfang@bjtu.edu.cn

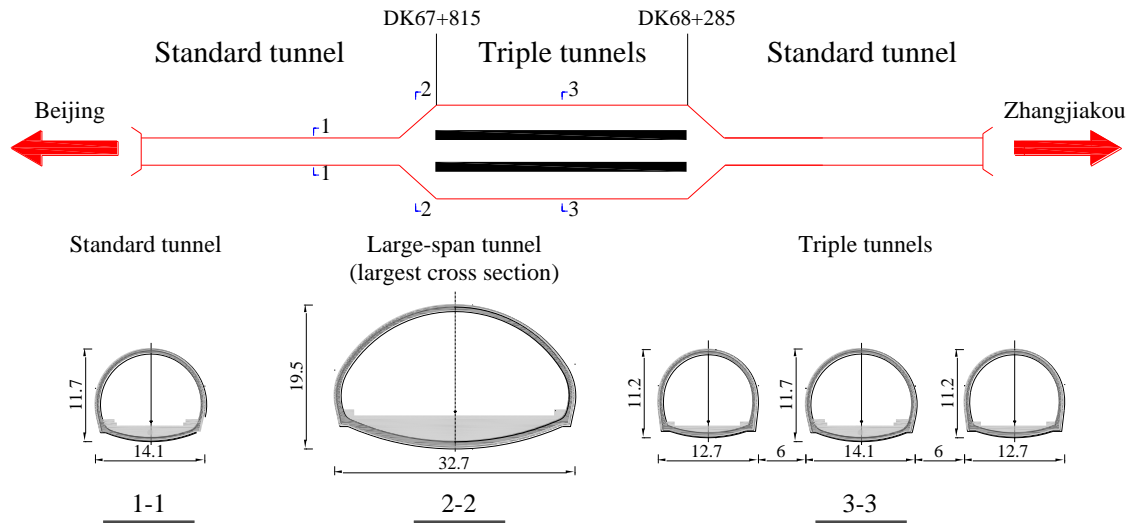


Fig. 1 Layout and typical cross section of new Badaling tunnel (unit: m)

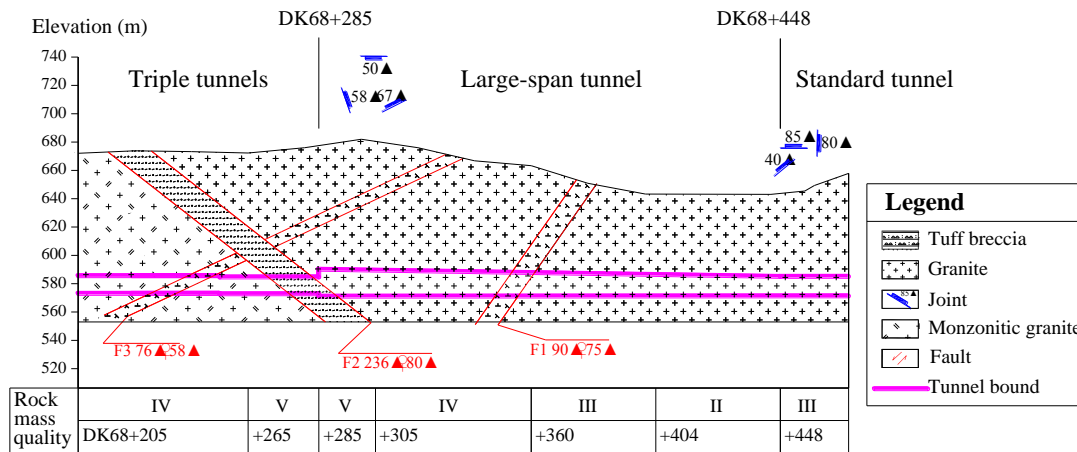


Fig. 2 Geological profile of large-span tunnel

under construction between Beijing and Zhangjiakou in China, of which the total length is approximately 174 km. The project serves for the 2022 Winter Olympics to be held in Beijing and Zhangjiakou. The Badaling tunnel, with a length of 12.0 km (from DK59+260 to DK71+270), is the longest tunnel project of the Beijing-Zhangjiakou high-speed railway. The overburden depth of the Badaling tunnel varies from 4 m to 432 m. The tunnel is excavated below the Badaling Great Wall for two times (at DK67+370 and DK67+025), which may bring negative impacts on the historical wall. The tunnel near the Badaling station (from DK67+815 to DK68+285) is composed of three types of the tunnel: triple tunnels, large-span tunnel with different cross-sections, and standard double-track single-tube tunnel (Fig. 1).

Fig. 2 shows the typical geological profile of the large-span tunnel from DK68+285 to DK68+448. The rock mass is generally intact with only 3-4 sets of joints largely developed. The joint fractures are considerable. The tunnel passes through a large fault and fracture zone (F2) and two small faults and fracture zones (F1, F3), with abundant groundwater.

The maximum height and span of the large-span tunnel are 19.5 m and 32.7 m, respectively, of which the excavation sequence is shown in Fig. 3. The thicknesses of the primary and the secondary linings are 32 cm and 75 cm, respectively. Table 1 lists the simplified relationship between the rock mass quality of the Chinese classification basic quality (BQ) system and the widely used quality (Q) system (Zhang *et al.* 2013). Fig. 2 also shows the rock mass classification of the large-span tunnel.

Table 1 Relationship between BQ System and Q System

Class Parameter	Class I (very good)	Class II (good)	Class III (fair)	Class IV (poor)	Class V (very poor)
BQ	> 550	451~550	351~450	251~350	< 250
Q	> 40	10~40	4~10	1~40	< 1

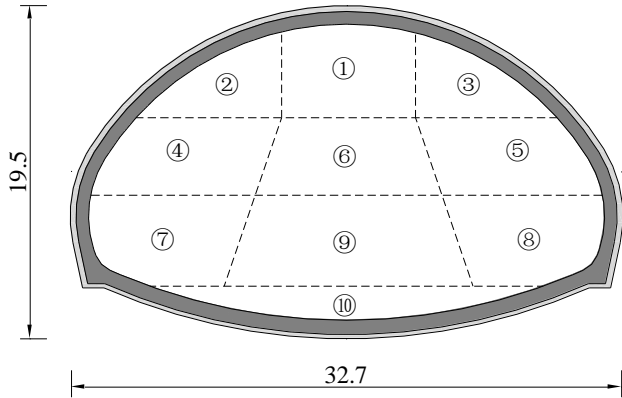


Fig. 3 Cross section of large-span tunnel (unit: m), the circle number indicating excavation

3. On-site monitoring

Microseismic monitoring technique, as an advanced and effective method for tunnel blast monitoring (Ye *et al.* 2013, Ye *et al.* 2014, Ye *et al.* 2018), has been widely applied to the monitoring of many tunnels (Grechka *et al.* 2015, Xiao *et al.* 2016). In this section, the microseismic monitoring scheme and related monitoring results of the large-span tunnel of the Badaling tunnel project are illustrated.

3.1 Monitoring system

The microseismic monitoring system comprises vibration transducers, data collectors, a fibre switch, a data storage server and a data processing system. Fig. 4 shows the network diagram of the microseismic monitoring system. Table 2 lists the monitoring devices and related performance parameters. Fibre switch is used to connect the microseismic collector and the remote monitoring terminal to achieve remote view and control.

Table 2 Monitoring devices and performance parameters

Device	Type	Parameter
Microseismic data collector	Three-channel data collector	Sampling rate: 2000 Hz; Trigger precision: $\pm 1 \mu s$ at all sample rates
Microseismic vibration transducer	Three-component transducer	Sensitivity: 200 V/m/s; Target acceptance frequency: 4.5–1000 Hz

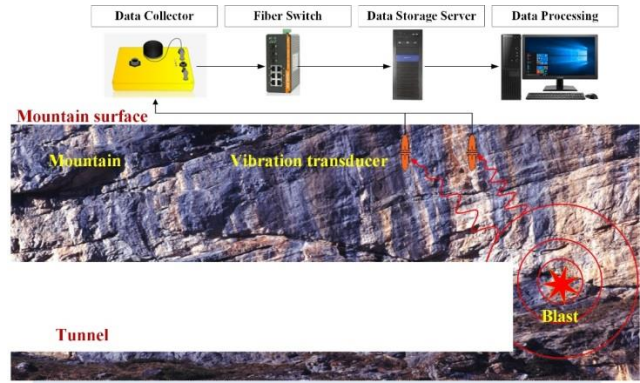


Fig. 4 Microseismic monitoring system network

3.2 Microseismic measuring points on mountain surface

A total of nine three-component transducers are installed on the mountain surface, each of which is accompanied by a three-channel data collector and a battery. The measuring points are numbered from 1# to 9#, and the measuring envelope is formed by taking 9# point at Dk68+365 as the centre with an 80 m radius (Fig. 5). The surface microseismic measuring holes are drilled at a depth of 2 m from surface. The diameter of the borehole is about 100 mm. Figs. 6 and 7 show the field installation photos.

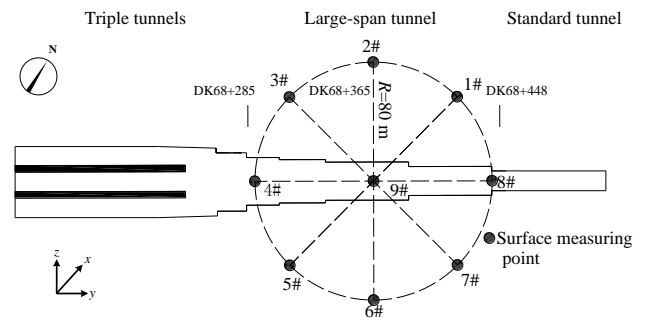


Fig. 5 Layout of measuring points on surface



Fig. 6 Installation of transducers on surface



Fig. 7 Data collector and battery

Table 3 Monitoring data of 3 sets of blast

ID	M_w	Point	R (m)	f_c (Hz)	x-PPV (cm/s)	y-PPV (cm/s)	z-PPV (cm/s)	Q (kg)	Rock mass class	
1	-0.1		1#	141.6	61	0.03854	0.02424	0.03642	120	II
			2#	144.9		0.04911	0.03193	0.04476		
			3#	133.6		0.06337	0.03894	0.04288		
			4#	118.5		0.04650	0.07474	0.04705		
			5#	98.9		0.03748	0.06694	0.07978		
			6#	137.4		0.04088	0.03023	0.02336		
			7#	132.5		0.04056	0.03856	0.02571		
			8#	112.9		0.07978	0.05417	0.06095		
			9#	98.2		0.07978	0.07978	0.07978		
2	-0.4		1#	104.2	100	0.02164	0.01700	0.01519	120	III
			2#	103.9		0.01349	0.01469	0.01727		
			3#	124.2		0.03312	0.02252	0.03124		
			4#	100.1		0.02160	0.04512	0.05387		
			5#	76.1		0.03544	0.04304	0.04169		
			6#	94.8		0.02275	0.02844	0.01837		
			7#	76.8		0.06611	0.07978	0.03862		
			8#	73.4		0.06389	0.06338	0.04652		
			9#	88		0.05256	0.06596	0.07978		
3	0.05	-	1#	123.4	94	0.01567	0.01835	0.01361	80	IV
			2#	124.4		0.01954	0.01482	0.01585		
			3#	101.3		0.02800	0.02252	0.03162		
			4#	109.3		0.02644	0.03503	0.02735		
			5#	83.6		0.02374	0.02655	0.02688		
			6#	113.3		0.02104	0.01688	0.01448		
			7#	85.5		0.03879	0.03333	0.03575		
			8#	80.6		0.05054	0.07978	0.06957		
			9#	84.6		0.06254	0.03422	0.07978		

3.3 Monitoring results

Based on the microseismic monitoring system, parameters including PPV, blast charge (Q), distance from the blast point to the mountain surface (R), corner frequency (f_c), and moment magnitude (M_w) can be obtained. The microseismic monitoring results due to 53 times of blast inside the large-span tunnel are collected and analyzed. The number of times of blast under Class II, III, and IV rock

mass conditions are 16, 18, and 19, respectively. Table 3 lists 3 sets of the microseismic monitoring data on the surface obtained by blast in typical rock mass conditions.

4. Analysis of measured data of peak particle velocity (PPV)

4.1 Sadovskii-formula regression analysis method

For evaluation and control of the seismic effect of blasting operations, the most commonly used equation is that of M.A. Sadovskii. Sadovskii's equation defines the alteration in the velocity of rock mass vibration depending on the distance, the quantity of explosives, blasting conditions and geological characteristics of the rock mass, and it is determined based on trial blasting for a specific work environment (Sadovskii 1973, Lutovac *et al.* 2018). Thus in tunnel engineering, the results of field vibration monitoring are usually analyzed based on the regression analysis using the Sadovskii-formula, which is an empirical formula derived by considering a significant amount of measured data and using the similar law principle, that is

$$V = K \cdot \left(\frac{\sqrt[3]{Q}}{R} \right)^\alpha \tag{1}$$

where V is the vibration velocity of the particle (cm/s); Q is the total blast charge (kg); R is the distance from the blast point to the mountain surface (m); and the parameters K and α are related to the specific site conditions.

Eq. (1) can be transformed into Eq. (2), that is

$$\ln V = \ln K + \alpha \cdot \ln \left(\frac{\sqrt[3]{Q}}{R} \right) \tag{2}$$

Substituting $Y = \ln V$, $b = \ln K$, and $X = \ln(Q^{1/3}/R)$ into Eq. (2), a linear Eq. (3) can be obtained

$$Y = b + \alpha \cdot X \tag{3}$$

Based on a large amount of measured data, linear regression analysis is used to obtain a linear relationship between Y and X data. The parameters K and α can then be obtained.

4.2 Analysis of PPV data measured on surface

The PPV has been reported as either the 'maximum vector sum' (vector sum using maximum of each component regardless of time), the 'peak component particle velocity' (the maximum value in any direction), or the 'peak true resultant particle velocity' (summing the three orthogonal components coincident with time) (Sharif 2000). The maximum vector sum is now discouraged as it includes an unknown factor of safety. The peak component particle velocity is widely used for the assessment as the majority guide values are expressed in this form (BS 7385: part 2, 1993). In this research, we use the peak true resultant particle velocity to represent PPV for analysis.

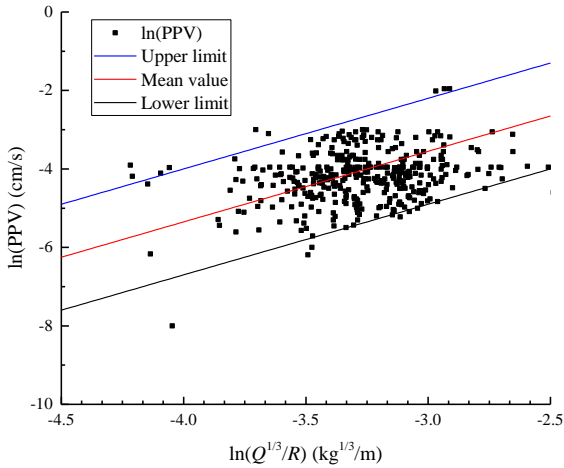


Fig. 8 Fitting curve between ln(PPV) and ln(Q^{1/3}/R)

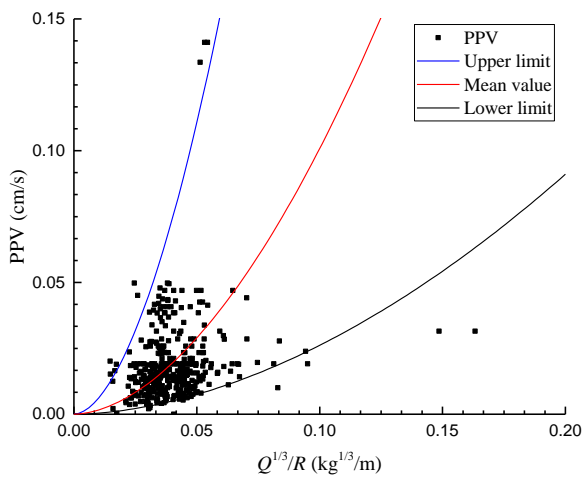


Fig. 9 Fitting curve between PPV and Q^{1/3}/R

A total of 447 sets of PPV data were collected from the 53 times of blast inside the large-span tunnel. The fitting curves between ln(PPV) and ln(Q^{1/3}/R), and between PPV and Q^{1/3}/R, obtained using the Sadosvskii-formula regression analysis method, are shown in Figs. 8 and 9, respectively. More than 99.5 percent of measuring data is bounded by the upper and lower bounds. The fitting parameters of the upper bound, the lower bound, and the mean value curves are shown in Table 4. The mean value formula can be used to predict the PPV due to blast vibration.

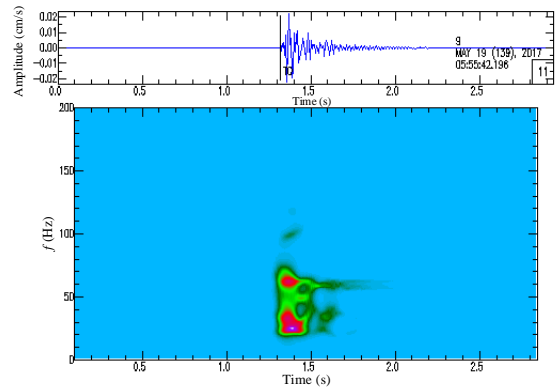
5. Frequency analysis of blast vibration

The effects on the Great Wall induced by blast inside tunnel should be evaluated considering the magnitude, frequency and duration of recorded vibration. If the resonant frequency of the Great Wall is close to the excitation frequency, the dynamic magnification of the structure may occur. In addition, a frequency-based vibration criterion is commonly adopted to evaluate the vibration effects.

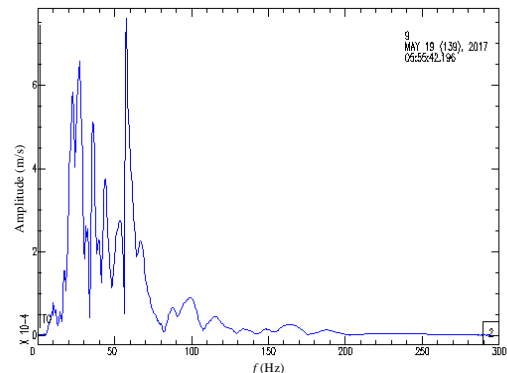
5.1 Corner frequency of blast vibration

The blast signal is processed using microseismic analysis software. The waveform diagram, time-frequency analysis diagram, and spectrum analysis diagram of a typical blast are shown in Fig. 10. The time duration of a blast varies from 1.3 to 2.0 s. The frequency of a blast is in the range of 20 to 80 Hz, of which the frequency of the predominant pulse (corner frequency) is 60 Hz.

The distribution of the corner frequency of the 53 sets of blast signal is shown in Fig. 11. The frequency ranges from 40 to 140 Hz, of which 75.1% sets of data are in the range of 60-110 Hz.



(a) Waveform and time-frequency analysis



(b) Spectrum analysis

Fig. 10 Blasting signal

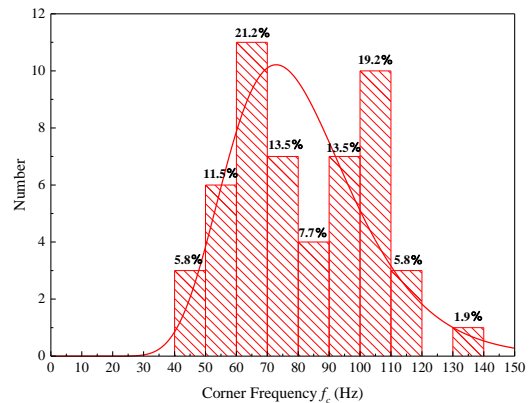


Fig. 11 Distribution of corner frequency of blasting

Table 4 Fitting results of PPV

	Upper limit formula	Mean formula	Lower limit formula
Linear fitting of Y and X	$Y = 1.8 \cdot X + 3.2$	$Y = 1.8 \cdot X + 1.85$	$Y = 1.8 \cdot X + 0.5$
Fitting of PPV	$PPV = 24.53 \cdot \left(\frac{\sqrt[3]{Q}}{R}\right)^{1.8}$	$PPV = 6.36 \cdot \left(\frac{\sqrt[3]{Q}}{R}\right)^{1.8}$	$PPV = 1.65 \cdot \left(\frac{\sqrt[3]{Q}}{R}\right)^{1.8}$

Table 5 Prediction formula of corner frequency under different rock mass conditions

Rock mass class	Values β	Prediction formula of corner frequency
Class II	13000	$f_c = \frac{13000}{\pi \cdot R} \ln\left(\frac{R^{1.3}}{1.65 \cdot Q^{0.6}}\right)$
Class III	12000	$f_c = \frac{12000}{\pi \cdot R} \ln\left(\frac{R^{1.3}}{1.65 \cdot Q^{0.6}}\right)$
Class IV	10000	$f_c = \frac{10000}{\pi \cdot R} \ln\left(\frac{R^{1.3}}{1.65 \cdot Q^{0.6}}\right)$

5.2 Analysis of influencing factors of corner frequency

The corner frequency generated by blast is closely related to many factors, such as the distance between the monitoring point and the blast location (R), the total blast charge (Q), and the propagation parameters of the rock mass. To investigate the factors that influence the corner frequency, we propose a new formula by combining the formula proposed by Ricker (1977) and the Sadovskii formula (1973), that is

$$f_c = \frac{\beta}{\pi R} \ln\left(\frac{R^{\alpha-1/2}}{K \cdot Q^{1/3\alpha}}\right) \tag{4}$$

where β is the absorption factor of the rock mass. According to the results of the previous calculation, the parameters $K=1.65$ and $\alpha=1.8$ are used. Accordingly, the corner frequency equation can be rewritten as follows

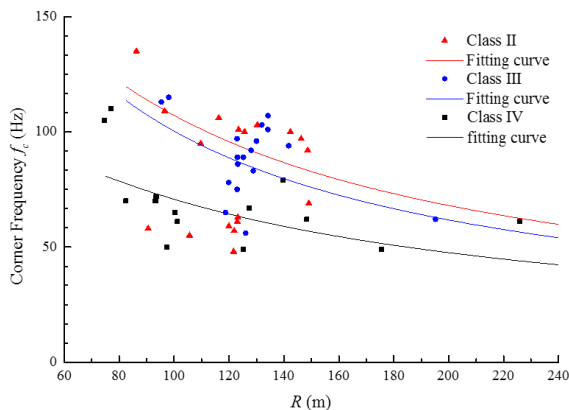


Fig. 12 Relationship between R and f_c under different rock mass class conditions

$$f_c = \frac{\beta}{\pi R} \ln\left(\frac{R^{1.3}}{1.65 \cdot Q^{0.6}}\right) \tag{5}$$

The relationships between R and f_c under different rock mass conditions can be obtained by fitting the measured data, which are shown in Fig. 12. The formulas of corner frequencies under different rock mass conditions are shown in Table 5.

6. Safety assessment of blast construction

6.1 Assessment of vibration velocity of the Great Wall

The safety assessment of the blast vibration of buildings adjacent to tunnel should be based on simultaneous consideration of the PPV and the corner frequency. Moreover, considering the historic and sensitive buildings near the blast construction, the PPV on the mountain surface should be strictly controlled. Different countries have employed different criteria of blast vibration to protect historic and sensitive buildings (Dowding 1992, Lu *et al.* 2012, GB6722-2014 2014), which are shown in Table 6.

According to the analysis of the measured data above, the corner frequency due to blast is largely concentrated in the range of 60-100 Hz, and the maximum PPV of the surface is 0.15 cm/s. Referring to the Chinese standards shown in Table 6, the measured values of PPV are clearly lower than the allowable values, indicating that the tunnel blast inside tunnel has minor effects on the Great Wall.

Table 6 Safety standards of blasting vibration velocity for protecting building in several countries

Country	Protection type	Safety standard of blasting vibration velocity (cm/s)		
China	Historic buildings	< 10 Hz	10 Hz~50 Hz	50 Hz~100 Hz
		0.1~0.2	0.2~0.3	0.3~0.5
Germany	Sensitive buildings	< 10 Hz	10Hz~50Hz	50 Hz~100 Hz
		0.3	0.3~0.8	0.8~1.2
Switzerland	Historic and sensitive older buildings	10 Hz~60 Hz		60 Hz~90 Hz
		0.8		0.8~1.2
India	Older buildings	<8 Hz	8 Hz~25 Hz	>25 Hz
		0.2	0.5	1

6.2 Assessment of resonance safety of the Great Wall

Resonance is the tendency of a mechanical system to absorb more energy when the frequency of its oscillations matches the system's natural frequency of vibration than it does at other frequencies. It may cause violent swaying motions to the concerned structures. A sketch of the cross section and a photo of the Great Wall are shown in Fig. 13.

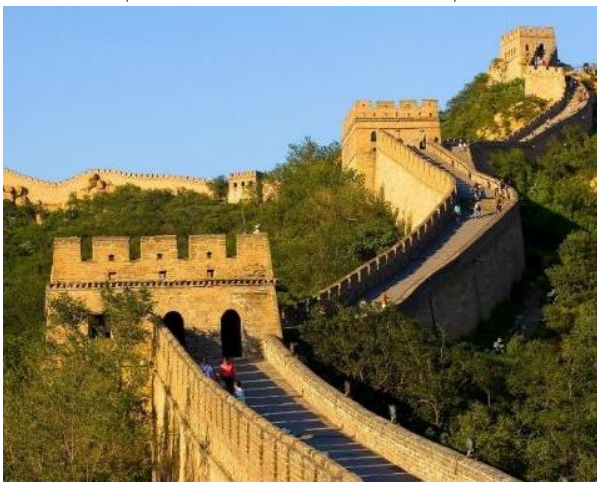
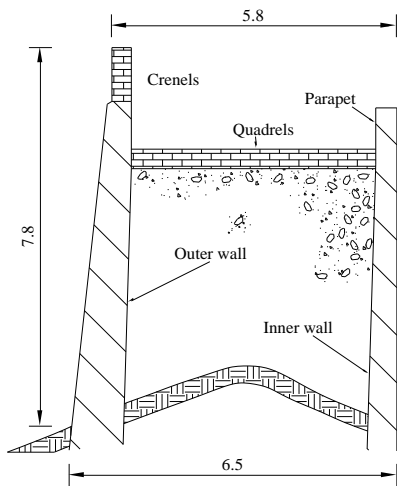


Fig. 13 Sketch of the cross section and photo of the Great Wall (unit: m)

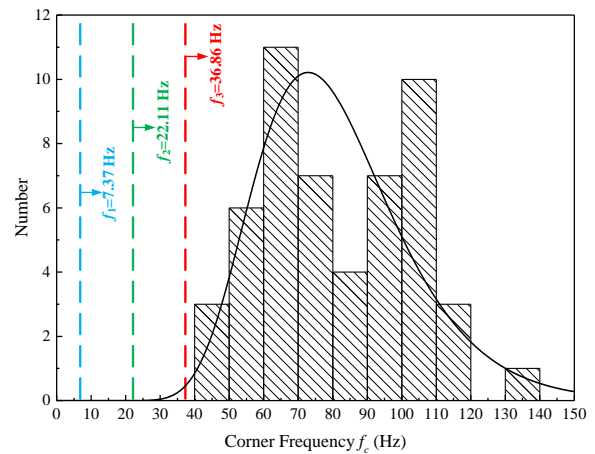


Fig. 14 Recorded corner frequencies of blasting signal and natural frequencies of the Great Wall

According to the Chinese code (GB/T50452-2008 2008), the Great Wall can be considered as a single-storey masonry structure. The *i*th order natural frequency of the Great Wall (*f_i*) can be expressed as follows

$$f_i = \frac{1}{2\pi H} \lambda_i \psi \tag{6}$$

where *H* is the height of the structure. The value of the parameter ψ is 230 m/s, which is obtained by table lookup. The values of the parameters λ_1 , λ_2 , and λ_3 of the structure, which are also determined by table lookup, are 1.571, 4.712, and 7.854 respectively. Therefore, the first three orders of the natural frequency of the Great Wall are 7.37, 22.11, and 36.86 Hz respectively.

The first three orders of natural frequencies of the Great Wall and the recorded corner frequencies due to blast inside tunnel are shown in Fig. 14. We can see the values of the recorded frequencies are larger than the values of the first three orders of natural frequencies of the Great Wall. This means the blast inside tunnel will not cause resonance problems.

7. Conclusions

The new Badaling tunnel is excavated below the Badaling Great Wall using the drilling and blast method.

The vibration due to blast inside the tunnel is a source of concern for the safety of the Great Wall. To assess the effects of the imposed vibration on the Great Wall, the microseismic monitoring technique is adopted to record the PPV and corner frequency on the mountain surface.

The recorded PPV values are lower than the guide value (0.3 cm/s) in the frequency range of the predominant pulse (from 40 Hz to 140 Hz). Meanwhile, the measured corner frequency of due to blast is larger than the natural frequencies of the Great Wall, which will not lead to resonant vibration of the Great Wall. Therefore, it is concluded that the vibration safety of the Great Wall due to blast can be ensured.

Based on the microseismic monitoring data from mountain surface, a series of empirical formulas are obtained by regression analysis, which can be used to predict the PPV and the corner frequency of the mountain surface due to blast inside the tunnel. The proposed empirical formulas can be applied to determine the blast charge when the blast is performed adjacent to concerned structures.

Acknowledgments

The authors gratefully acknowledge the financial support by the Fundamental Research Funds for the Central Universities under Grant 2016JBZ009.

References

- Ak, H., Iphar, M., Yavuz, M. and Konuk, A. (2009), "Evaluation of ground vibration effect of blast operations in a magnesite mine", *Soil Dyn. Earthq. Eng.*, **29**(4), 669-676.
- Aldas, G.G.U. (2010), "Explosive charge mass and peak particle velocity (ppv)-frequency relation in mining blast", *J Geophys. Eng.*, **7**(3), 223-231.
- Amnieh, H.B., Siamaki, A. and Soltani, S. (2012), "Design of blast pattern in proportion to the peak particle velocity (ppv): artificial neural networks approach", *Safety Sci.*, **50**(9), 1913-1916.
- Arora, S. and Dey, K. (2010), "Estimation of near-field peak particle velocity: a mathematical model", *J. Geol. Min. Res.*, **2**(4), 68-73.
- BS 7385: part 2 (1993), Evaluation and measurement for vibration in buildings, part 2 Guide to damage levels from groundborne vibration, British standards institution; London, British.
- Dargahi-Noubary, G.R. (1998), "Statistical estimation of corner frequency and its application to seismic event-identification", *Soil Dyn. Earthq. Eng.*, **17**(5), 297-309.
- Dehghani, H. and Ataee-Pour, M. (2011), "Development of a model to predict peak particle velocity in a blast operation", *Int. J. Rock Mech. Min. Sci.*, **48**(1), 51-58.
- Dowding, C.H. (1992), "Suggested method for blast vibration monitoring", *Int. J. Rock Mech. Min. Sci. Geomech. Abstr.*, **29**(2), 145-156.
- Faradonbeh, R.S., Armaghani, D.J., Majid, M.Z.A., Tahir, M.M., Murlidhar, B.R., Monjezi, M. and Wong, H.M. (2016), "Prediction of ground vibration due to quarry blast based on gene expression programming: a new model for peak particle velocity prediction", *Int. J. Environ. Sci. Technol.*, **13**(6), 1453-1464.
- GB6722-2014 (2014), Safety Regulations for Blast, China Standard Press; Beijing, China.
- GB/T50452-2008 (2008), Code for Anti-industrial Vibration of Ancient Structures, China Architecture & Building Press; Beijing, China.
- Grechka, V., Artman, B., Eisner, L., Heigl, W. and Wilson, S. (2015), "Microseismic monitoring-introduction", *Geophys.*, **80**(6), WCi-WCii.
- Hasanipanah, M., Faradonbeh, R.S., Amnieh, H.B., Armaghani, D. J. and Monjezi, M. (2017), "Forecasting blast-induced ground vibration developing a cart model", *Eng. Comput.*, **33**(2), 307-316.
- Jiang, N. and Zhou, C. (2012), "Blast vibration safety criterion for a tunnel liner structure", *Tunn. Undergr. Sp. Tech.*, **32**(6), 52-57.
- Li, L.P., Li, S.C., Zhang, Q.S., Wang, G. and Ma, F.K. (2008), "Monitoring blast excavation of shallow-buried large-span tunnel and vibration reduction technology", *Rock Soil Mech.*, **29**(8), 2292-2296 (in Chinese).
- Lu, W.B., Luo, Y. and Shu, D.Q. (2012), "An introduction to Chinese safety regulations for blast vibration", *Environ. Earth Sci.*, **67**(7), 1951-1959.
- Lu, W.B., Zhang, L., Zhou, J.R., Jin, X.H., Chen, M. and Yan, P. (2013), "Theoretical analysis on decay mechanism and law of blast vibration frequency", *Blast*, **30**(2), 1-7.
- Lutovac, S., Gluščević, B., Tokalić, R., Majstorović, J. and Beljić, Č. (2018), "Models of determining the parameters of rock mass oscillation equation with experimental and mass blastings", *Minerals*, **8**(2), 70-88.
- Monjezi, M., Ghafurikalajahi, M. and Bahrami, A. (2011), "Prediction of blast-induced ground vibration using artificial neural networks", *Tunn. Undergr. Sp. Tech.*, **26**(1), 46-50.
- Nateghi, R. (2012), "Evaluation of blast induced ground vibration for minimizing negative effects on surrounding structures", *Soil Dyn. Earthq. Eng.*, **43**(12), 133-138.
- New, B.M. (1986), "Ground vibration caused by civil engineering works", Transport and Road Research Laboratory Research Report 53:19
- Ricker, N.H. (1977), *Transient Waves in Visco-Elastic Media*, Elsevier Scientific Publishing Company, Amsterdam, The Netherlands.
- Sadovskii, M.A., Mel'Nikov, N.V. and Demidyuk, G.P. (1973), "The main trends in the development of blast techniques in mining", *Soviet Mining*, **9**(3), 257-264.
- Saiang, D. and Nordlund, E. (2009), "Numerical analyses of the influence of blast-induced damaged rock around shallow tunnels in brittle rock", *Rock Mech. Rock Eng.*, **42**(3), 421-448.
- Sambuelli, L. (2009), "Theoretical derivation of a peak particle velocity-distance law for the prediction of vibrations from blast", *Rock Mech. Rock Eng.*, **42**(3), 547-556.
- Sato, T. and Hirasawa, T. (1973), "Body wave spectra from propagating shear cracks", *J. Phys. Earth.*, **21**(4), 415-431.
- Sharif, A.K. (2000), "Dynamic performance investigation of base isolated structures", Ph.D. Dissertation, Imperial College London, London
- Verma, H.K., Samadhiya, N.K., Singh, M., Goel, R.K. and Singh, P. K. (2018), "Blast induced rock mass damage around tunnels", *Tunn. Undergr. Sp. Tech.*, **71**, 149-158.
- Wyss, M., Hanks, T.C. and Liebermann, R.C. (1971), "Comparison of p-wave spectra of underground explosions and earthquakes", *J. Geophys. Res.*, **76**(11), 2716-2729.
- Xia, X., Li, H., Liu, Y. and Yu, C. (2018), "A case study on the cavity effect of a water tunnel on the ground vibrations induced by excavating blasts", *Tunn. Undergr. Sp. Tech.*, **71**, 292-297.
- Xiao, Y.X., Feng, X.T., Hudson, J.A., Chen, B.R., Feng, G.L. and Liu, J.P. (2016), "Isrm suggested method for in situ microseismic monitoring of the fracturing process in rock masses", *Rock Mech. Rock Eng.*, **49**(1), 343-369.
- Yang, J., Lu, W., Jiang, Q., Yao, C., Jiang, S. and Tian, L. (2016),

- “A study on the vibration frequency of blast excavation in highly stressed rock masses”, *Rock Mech. Rock Eng.*, **49**(7), 2825-2843.
- Ye, X.W., Ni, Y.Q., Wai, T.T., Wong, K.Y., Zhang, X.M. and Xu, F. (2013), “A vision-based system for dynamic displacement measurement of long-span bridges: algorithm and verification”, *Smart Struct Syst.*, **12**(3), 363-379.
- Ye, X.W., Su, Y.H. and Han, J.P. (2014), “Structural health monitoring of civil infrastructure using optical fiber sensing technology: A comprehensive review”, *Sci. World J.*, **2014**, 652329, 1-11
- Ye, X.W., Xi, P.S., Su, Y.H., Chen, B. and Han, J.P. (2018), “Stochastic characterization of wind field characteristics of an arch bridge instrumented with structural health monitoring system”, *Struct Saf.*, **71**, 47-56.
- Zhang, D.L., Fang, Q., Hou, Y.J., Li, P.F. and Wong, L.N.Y. (2013), “Protection of buildings against damages as a result of adjacent large-span tunneling in shallowly buried soft ground”, *J. Geotech. Geoenviron. Eng.*, **139**(6), 903-913.